Presenilin 2 modulates endoplasmic reticulum (ER)–mitochondria interactions and Ca^{2+} cross-talk

Enrico Zampese[a], Cristina Fasolato[a], Maulilio J. Kipanyula[a], Mario Bortolozzi[b,c], Tullio Pozzan[a,b,d,1], and Paola Pizzo[a,1]

Departments of [a]Biomedical Sciences and [c]Physics, University of Padua, 35121 Padua, Italy; [b]Venetian Institute of Molecular Medicine, 35129 Padua, Italy; and [d]Consiglio Nazionale delle Ricerche Institute of Neuroscience, 35121 Padua, Italy

Contributed by Tullio Pozzan, January 14, 2011 (sent for review November 30, 2010)

Presenilin mutations are the main cause of familial Alzheimer's disease (FAD). Presenilins also play a key role in Ca^{2+} homeostasis, and their FAD-linked mutants affect cellular Ca^{2+} handling in several ways. We previously have demonstrated that FAD-linked presenilin 2 (PS2) mutants decrease the Ca^{2+} content of the endoplasmic reticulum (ER) by inhibiting sarcoendoplasmic reticulum Ca^{2+}-ATPase (SERCA) activity and increasing ER Ca^{2+} leak. Here we focus on the effect of presenilins on mitochondrial Ca^{2+} dynamics. By using genetically encoded Ca^{2+} indicators specifically targeted to mitochondria (aequorin- and GFP-based probes) in SH-SY5Y cells and primary neuronal cultures, we show that overexpression or down-regulation of PS2, but not of presenilin 1 (PS1), modulates the Ca^{2+} shuttling between ER and mitochondria, with its FAD mutants strongly favoring Ca^{2+} transfer between the two organelles. This effect is not caused by a direct PS2 action on mitochondrial Ca^{2+}-uptake machinery but rather by an increased physical interaction between ER and mitochondria that augments the frequency of Ca^{2+} hot spots generated at the cytoplasmic surface of the outer mitochondrial membrane upon stimulation. This PS2 function adds further complexity to the multifaceted nature of presenilins and to their physiological role within the cell. We also discuss the importance of this additional effect of FAD-linked PS2 mutants for the understanding of FAD pathogenesis.

fluorescent Ca^{2+} probe | intracellular organelle tethering | fluorescence resonance energy transfer

Alzheimer's disease (AD) is the most common form of dementia in developed countries. The pathogenesis of AD is still largely mysterious, and most basic research in the field is concentrated on rare genetic forms of familial AD (FAD). The majority of FAD cases are caused by point mutations in genes for two homologous proteins, presenilin 1 (PS1) and presenilin 2 (PS2), that are essential components of the γ-secretase complex responsible for the production of the amyloid β peptides (Aβ) (1).

Evidence has accumulated suggesting that FAD is linked to an imbalance of cellular Ca^{2+} homeostasis (see refs. 2 and 3 for recent reviews). In particular, presenilins appear to play a key role in the control of Ca^{2+} concentration within the endoplasmic reticulum (ER), $[Ca^{2+}]_{ER}$: (*i*) Several FAD-linked presenilin mutants altered the expression or sensitivity of ER Ca^{2+} release channels [ryanodine receptor (RyR) and inositol 1,4,5-trisphosphate receptor (IP_3R)] in cell lines, neurons, and brain microsomes (see ref. 4 for a recent review); (*ii*) the sarcoendoplasmic reticulum Ca^{2+} ATPase (SERCA) has been proposed as a target of presenilins, although opposite regulatory effects have been reported (5, 6); and (*iii*) it has been suggested that WT presenilins, but not FAD-linked presenilin mutants, form low-conductance Ca^{2+} leak channels in the ER membrane (7, 8). This last finding supports the "Ca^{2+} overload" hypothesis for FAD, which proposes that the reduced ER Ca^{2+} leak caused by FAD-linked presenilin mutants results in an increased $[Ca^{2+}]_{ER}$ and consequently an exaggerated Ca^{2+} release upon cell stimulation (9, 10). However, other groups have reported opposite results. In particular, the observation that, in various models, upon overexpression of FAD-linked presenilin mutants, an enhanced Ca^{2+} release occurs in the absence of ER Ca^{2+} overload moved attention from the $[Ca^{2+}]_{ER}$ to the hyperactivity of ER Ca^{2+} release channels (11–13). Along this line, a group of laboratories found that, in various cell systems, presenilin expression leaves unchanged or eventually reduces the steady-state $[Ca^{2+}]_{ER}$ (4).

Other organelles (e.g., the Golgi apparatus and mitochondria) appear to be targets of presenilin action. It has been reported recently (14) that presenilins are enriched in ER mitochondria-associated membranes, i.e., the ER membrane domains interacting closely with mitochondria and endowed with key players of the Ca^{2+}-handling machinery (15). This finding, together with the generally accepted concept that mitochondrial deficits are key events in most neurodegenerative diseases (16, 17), and more specifically in AD (18, 19), led us to investigate the effect of presenilins on ER–mitochondria cross-talk.

By directly measuring mitochondrial Ca^{2+} dynamics, we show here that PS2, but not PS1, favors Ca^{2+} transfer between ER and mitochondria, an effect reduced by PS2 down-regulation and enhanced by the expression of PS2 mutants. The most striking modification associated with PS2 expression is an increased number of contact sites between ER and mitochondria. The physiological role of PS2 in tethering the two organelles and the pathological consequences of this additional function, are discussed.

Results

PS2 Expression Increases Mitochondrial Ca^{2+} Uptake. We have shown previously that PS2 overexpression results in a partial depletion of intracellular Ca^{2+} stores because of reduced SERCA activity and increased Ca^{2+} leak (6, 20). As a consequence, the maximal amplitude of cytosolic Ca^{2+}, $[Ca^{2+}]_c$, rises, due to mobilization from intracellular stores, is reduced. The question then arises as to the consequences of this PS2 effect on other cellular functions, in particular on mitochondrial Ca^{2+} homeostasis, given its importance for energy metabolism and cell-death control.

Cells from the SH-SY5Y neuroblastoma line were cotransfected with the cDNA for PS2 (WT or the FAD mutant PS2-T122R) together with cDNA coding for either cytosolic-targeted aequorin (cyt-Aeq) or mitochondria-targeted aequorin (mit-Aeq). Fig. 1*A* shows the results of a typical experiment in which SH-SY5Y cells in a Ca^{2+}-free medium were exposed to maximal stimulatory doses (100 nM) of the IP_3-generating agonist bradykinin (BK) together with 20 μM of the SERCA inhibitor cyclopiazonic acid (CPA) to induce a prompt and complete release of Ca^{2+} from intracellular stores. Cells overexpressing PS2 (Fig. 1*A*, black trace) showed a reduced mitochondrial Ca^{2+}, $[Ca^{2+}]_m$, peak compared to controls (Fig. 1*A*, gray trace), as expected from the reduced $[Ca^{2+}]_c$ rise (Fig. 1, *Inset*, and refs. 6

Author contributions: C.F., T.P., and P.P. designed research; E.Z. and M.J.K. performed research; M.B. contributed new reagents/analytic tools; E.Z., C.F., T.P., and P.P. analyzed data; and T.P. and P.P. wrote the paper.

The authors declare no conflict of interest.

Freely available online through the PNAS open access option.

[1]To whom correspondence may be addressed. E-mail: tullio.pozzan@unipd.it or paola.pizzo@unipd.it.

This article contains supporting information online at www.pnas.org/lookup/suppl/doi:10.1073/pnas.1100735108/-/DCSupplemental.

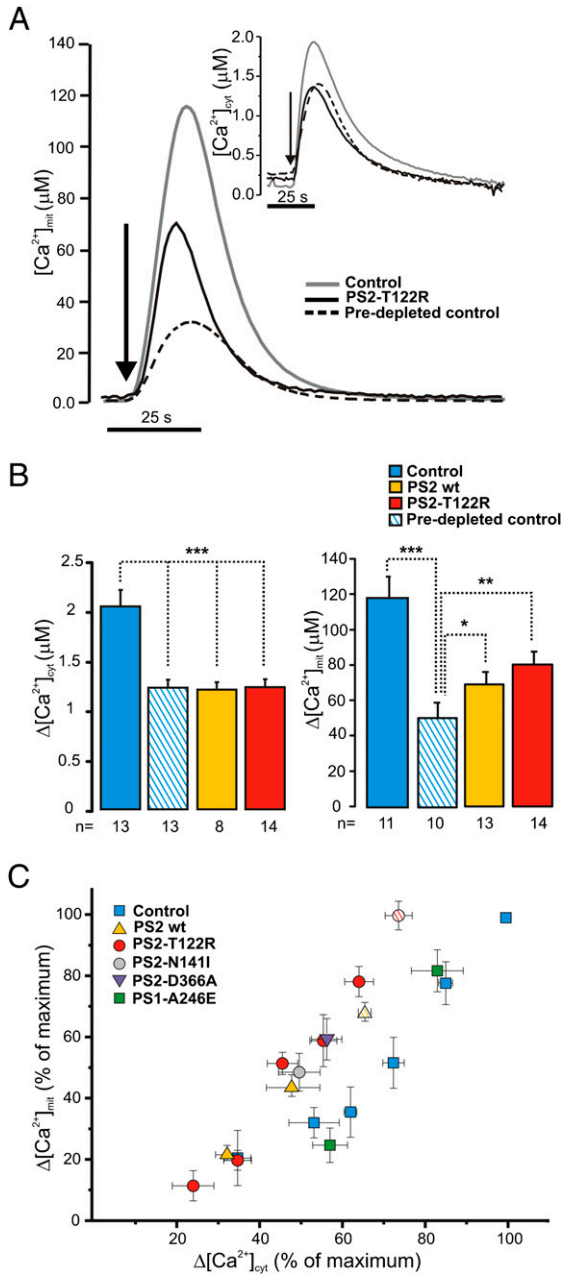

Fig. 1. Effects of PS2 overexpression on $[Ca^{2+}]_c$ and $[Ca^{2+}]_m$ changes in SH-SY5Y cells. SH-SY5Y cells were transfected with mit-Aeq or cyt-Aeq and with PS2 WT, PS2-T122R, or the void vector (control). Predepleted control cells were preincubated at 4 °C in a Ca^{2+}-free, EGTA-containing medium for 30 min. (*A*) Representative traces in control (gray line), predepleted control cells (dashed line), and PS2-T122R–expressing cells (black line) bathed in Ca^{2+}-free, EGTA-containing medium and challenged with CPA (20 μM) plus BK (100 nM). (*B*) Bars represent mean $[Ca^{2+}]_c$ (*Left*) and $[Ca^{2+}]_m$ (*Right*) upon stimulation in the different conditions (mean ± SEM; $*P < 0.05$; $**P < 0.01$; $***P < 0.001$; unpaired Student's *t* test; *n* = number of independent experiments). (*C*) Changes in $[Ca^{2+}]_m$ responses in controls (blue squares), cells expressing PS2 WT (yellow triangles) and cells expressing PS2-T122R (red circles) are plotted as a function of the corresponding changes in $[Ca^{2+}]_c$ peaks. Data are expressed as percentage (mean ± SEM) of the maximal change obtained in control cells of the same batch ($n = 20$, number of independent batches) stimulated as shown in *A*. For presentation, cytosolic data were binned (bin size 10%, observed frequency 3–10). Paired data obtained in cells expressing PS1-A246E (green squares), PS2-N141I (gray circles), or PS2-D366A (purple triangles) are included also. Data from cells overexpressing SERCA2b are indicated by hatched symbols.

and 20). The percentage decrease of the $[Ca^{2+}]_m$ peak was similar to or even smaller than that observed in the cytoplasm (Fig. 1*B*). This result was unexpected, given that mitochondria should amplify the decrease in $[Ca^{2+}]_c$ peaks; namely, a 20% drop in $[Ca^{2+}]_c$ should correspond to about a 40% decrease in $[Ca^{2+}]_m$ (21).

To address this point further, intracellular Ca^{2+} stores of control cells were partially depleted by preincubation in a Ca^{2+}-free medium containing EGTA (*Methods*). When the amplitude of $[Ca^{2+}]_c$ peaks of predepleted cells was brought close to that of cells overexpressing PS2 (Fig. 1*A*, *Inset*, and Fig. 1*B*, *Left*), the corresponding $[Ca^{2+}]_m$ peaks (Fig. 1*A*, dashed line) were substantially smaller than those of cells overexpressing PS2 (Fig. 1*A*, black line). On average, $[Ca^{2+}]_m$ peaks in PS2 overexpressing cells were 30% larger than those of predepleted controls (Fig. 1*B*, *Right*).

The relationship between $[Ca^{2+}]_c$ and $[Ca^{2+}]_m$ was investigated by a different approach. Cells were loaded with the ester form of the Ca^{2+} chelator EGTA (*Methods*) to decrease the amplitude of $[Ca^{2+}]_c$ peaks progressively without modifying $[Ca^{2+}]_{ER}$. Again, cells overexpressing PS2 showed higher $[Ca^{2+}]_m$ increases than seen in controls with similar $[Ca^{2+}]_c$ peaks (increases of 20 ± 8% for PS2 WT and 25 ± 7% for PS2-T122R; mean ± SEM; $n = 4$).

In Fig. 1*C* all paired data of $[Ca^{2+}]_c$ and $[Ca^{2+}]_m$ peaks in different experimental conditions (i.e., before depletion by incubation in Ca^{2+}-free medium or EGTA loading) were pooled. In cells overexpressing PS2, independently of the methodology used to reduce $[Ca^{2+}]_c$ peaks, $[Ca^{2+}]_m$ increases were larger than those in controls with similar $[Ca^{2+}]_c$ rises. The largest peaks were obtained only in controls, given that cells expressing PS2 never reached those $[Ca^{2+}]_c$ values. To maximize the $[Ca^{2+}]_c$ peaks of cells overexpressing PS2, SH-SY5Y cells were cotransfected with SERCA2b (6). Under these conditions, $[Ca^{2+}]_c$ peaks were increased but did not reach the values of control cells. The $[Ca^{2+}]_m$ rises also increased and approached those of controls (hatched symbols in Fig. 1*C*).

Taken together, these data indicate that PS2 overexpression, despite reducing the store Ca^{2+} content and thus $[Ca^{2+}]_c$ peaks, had an additional effect on mitochondria: It improved their capacity to take up Ca^{2+}. A possible explanation for such an effect of PS2 would be an increase in the intrinsic capacity of mitochondria to take up Ca^{2+}. We explored this possibility by measuring mitochondrial Ca^{2+} uptake in digitonin-permeabilized cells bathed with an intracellular-like buffer set at different Ca^{2+} levels (*SI Methods* and Fig. S1). Under these conditions, the $[Ca^{2+}]_m$ peaks and the rates of Ca^{2+} uptake were not statistically different in control cells, cells expressing PS2 WT, and cells expressing PS2-T122R.

PS2-T122R Increases the Number of Cells with High Mitochondrial Ca^{2+} Response. In the next series of experiments, $[Ca^{2+}]_c$ and $[Ca^{2+}]_m$ peaks were analyzed in single cells upon coexpression of PS2 (WT or mutant) together with two GFP-based Ca^{2+} probes: 4mtD1cpv, targeted to the mitochondrial matrix, and H2BD1cpv, targeted to the nucleoplasm (22). Because the two probes have clear and distinct cell localizations, nuclear and mitochondrial Ca^{2+} changes can be monitored in the same cell. The nuclear probe can be used as a surrogate for a cytosolic indicator, because the Ca^{2+} rises are similar in nucleoplasm and cytosol (22).

After cotransfection of H2BD1cpv, 4mtD1cpv, and PS2 (WT, T122R or the void vector), SH-SY5Y cells were challenged in a Ca^{2+}-free, EGTA-containing medium with a mixture of IP_3-generating agonists to discharge Ca^{2+} stores maximally. For each cell, the Ca^{2+} peak [increase in ratio (ΔR) normalized to the initial value (R_0), ($\Delta R/R_0$)] within the mitochondrial matrix then was plotted as a function of the corresponding increase in the nucleoplasm (Fig. 2*A*). The mitochondrial response of controls (blue diamonds in Fig. 2*A*) varied from a marginal (or no) increase to

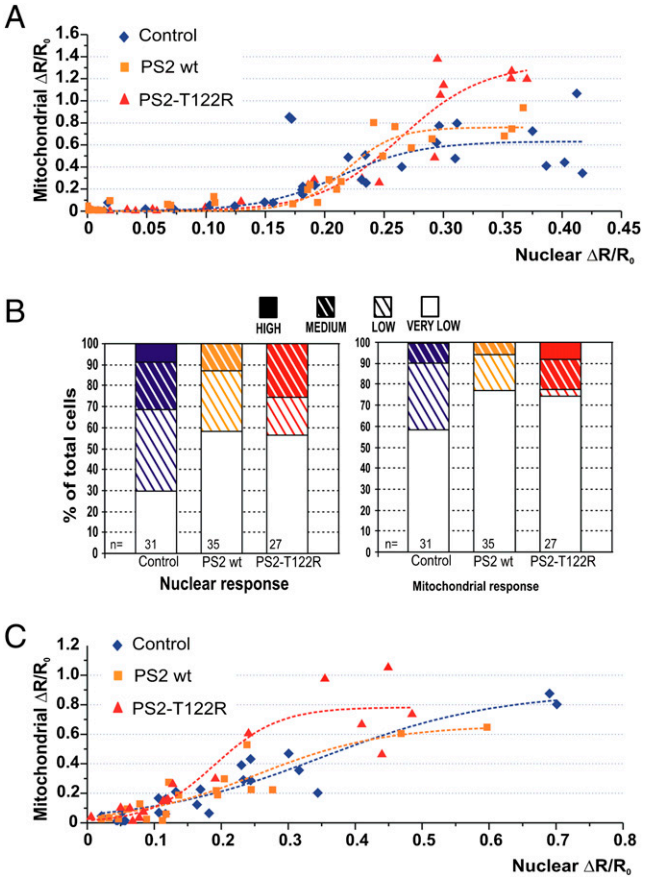

Fig. 2. Increases in nuclear and mitochondrial Ca^{2+} concentration in single SH-SY5Y cells and rat cortical neurons. Cells coexpressing H2BD1cpv, 4mtD1cpv, and: PS2 WT (yellow squares), PS2-T122R (red triangles), or void vector (control, blue diamonds) were stimulated in a Ca^{2+}-free, EGTA-containing medium with a mixture of IP_3-generating agonists (100 nM BK, 100 μM ATP, and 100 μM CCH). (*A*) The increase in $[Ca^{2+}]_m$ peak ($\Delta R/R_0$, normalized increase in ratio, ΔR, measured above the initial value, R_0) is plotted as a function of the corresponding increase in the nuclear Ca^{2+} peak in the same cell. (*B*) Based on the maximal value of $\Delta R/R_0$ obtained with each probe, cells were binned in four groups as very low-, low-, medium-, and high-responding cells, with bin size equal to 0.13 and 0.4 $\Delta R/R_0$ for nucleoplasm (≤0.13, ≤0.26, ≤0.39, and >0.39) and mitochondria (≤0.4, ≤0.8, ≤1.2, and >1.2), respectively. *n* = number of cells. (*C*) Primary rat cortical neurons coexpressing H2BD1cpv, 4mtD1cpv and: PS2 WT (yellow squares), PS2-T122R (red triangles), or void vector (control, blue diamonds) were stimulated in Ca^{2+}-free, EGTA-containing medium with a mixture of agonists [100 μM glutamate, 100 μM ATP, and 100 μM charbacol (CCH)] or 1 μM ionomycin. The increase in $[Ca^{2+}]_m$ peak is plotted as a function of the corresponding increase in the nuclear peak. Note that the $\Delta R/R_0$ values in *A* and *C* are different because two different imaging systems have been used (*SI Methods*).

a robust response, with a threshold at about 30% of the maximal nuclear response. In cells overexpressing PS2 WT (yellow squares in Fig. 2*A*), the pattern of $[Ca^{2+}]_m$ peaks was similar to that in controls, whereas in cells expressing the mutant PS2 (red triangles in Fig. 2*A*), large $[Ca^{2+}]_m$ peaks were found at nuclear Ca^{2+} rises eliciting smaller $[Ca^{2+}]_m$ responses in controls. In terms of cell number, when considering the nuclear response, overexpression of WT or mutant PS2 almost doubled the percentage of very-low-responding cells without reaching the high responses observed in controls. Conversely, at the mitochondrial level, the percentage of high-responding cells ($\Delta R/R_0$ >1.2) was larger in cells overexpressing PS2-T122R but was similar in controls and cells overexpressing PS2 WT (Fig. 2*B*). The same pattern was observed in rat cortical neurons: For similar increases in nuclear Ca^{2+}, the corresponding $[Ca^{2+}]_m$ peaks elicited by a mixture of IP_3-generating stimuli or ionomycin were larger in cells expressing PS2-T122R than in controls or in cells expressing PS2 WT (Fig. 2*C*). Thus, despite the large scatter of the single-cell data, the overall pattern is similar to that observed in cell-population measurements with aequorins.

PS2-T122R Increases Physical and Functional Interactions Between ER and Mitochondria. Plenty of evidence indicates that the rapid Ca^{2+} uptake into mitochondria upon Ca^{2+} release depends on close interactions of the organelles with the ER (23). The ER–mitochondria interactions thus were investigated in SH-SY5Y cells coexpressing WT or mutant PS2 together with a mitochondria-targeted RFP (mit-RFP) and an ER-targeted GFP (ER-GFP). When expressed in SH-SY5Y cells, neither PS2 WT nor PS2-T122R had any effect on the coarse distribution and morphology of the mitochondrial/ER network, as shown by *z*-projections of confocal stacks of cells expressing ER-GFP and mit-RFP (Fig. S2). However, significant differences were found when the regions of tethering were assessed quantitatively. As shown in Fig. 3 *A–C*,

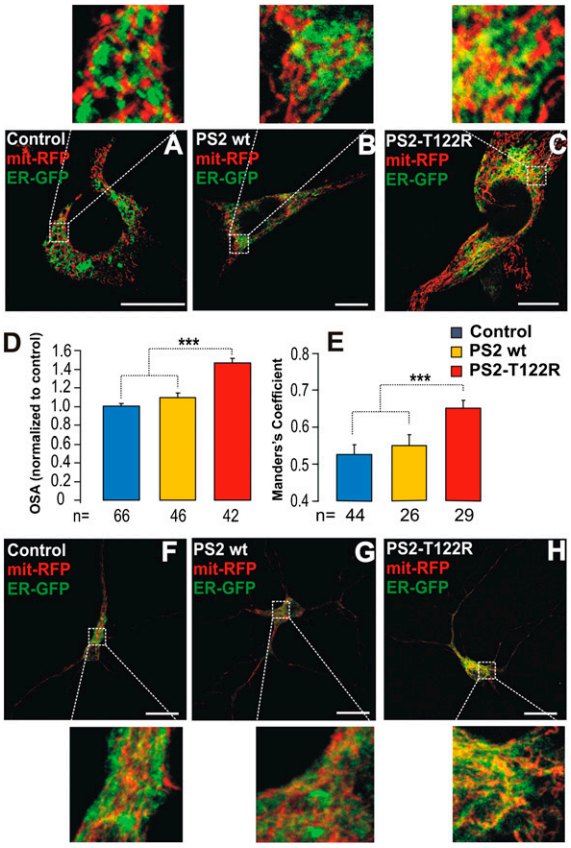

Fig. 3. ER–mitochondria interactions in SH-SY5Y cells and rat cortical neurons overexpressing PS2. (*A–C*) Confocal images of SH-SY5Y cells coexpressing a mitochondria-targeted RFP (mit-RFP) and an ER-targeted GFP (ER-GFP) together with the void vector (*A*), PS2 WT (*B*), or PS2-T122R (*C*). Cells were excited separately at 488 nm or at 543 nm, and the single images were recorded. The merging of the two images is shown for each condition. (Scale bar: 10 μm.) (*D*) Statistical quantification of the overlapping signal area (OSA), calculated from single confocal images and (*E*) Manders' coefficient for colocalization, calculated from *z*-axis confocal stacks, for each condition (mean ± SEM). ***$P < 0.001$; unpaired Student's *t* test; n = number of cells. (*F–H*) Rat cortical neurons treated as in *A–C*. For these cells, Manders' coefficient was 0.74 ± 0.027, 0.77 ± 0.02, and 0.84 ± 0.012 for controls (*n* = 34), PS2 WT (*n* = 30), and PS2-T122R–expressing (*n* = 29) cells, respectively. Data are shown as mean ± SEM; $P < 0.01$. (Scale bar: 10 μm.)

as compared with controls ($n = 66$), the area of colocalization (yellow) was increased in cells overexpressing either WT or mutant PS2. The effect was modest with PS2 WT (+9 ± 4.6%) but was much larger with PS2-T122R (+48 ± 6%) (Fig. 3*D*). Manders' colocalization coefficient (24), calculated from *z*-axis confocal stacks, revealed a significant increase in the ER–mitochondria juxtaposition only upon overexpression of PS2-T122R (Fig. 3*E*). Similar results were obtained in rat cortical neurons (Fig. 3 *F–H*).

Overexpression experiments might reveal functional aspects not shared by the endogenous protein under investigation. To test this possibility, SH-SY5Y cells were transfected with a siRNA specific for PS2 (*Methods*) or with a nonrelated siRNA as control. The PS2-specific siRNA caused a net decrease (−79 ± 14%; $n = 3$) of the endogenous PS2 level (Fig. 4*C*). Abating endogenous PS2 resulted in a significant decrease in the area of ER–mitochondria interaction (−20.5 ± 6.7% of control; mean ± SEM; $n = 20$; $P < 0.05$ (Fig. 4 *A* and *B*). We then tested the effect of endogenous PS2 down-regulation on $[Ca^{2+}]_c$ and $[Ca^{2+}]_m$ responses. The cytosolic response was unaffected, but the $[Ca^{2+}]_m$ increase was reduced significantly (−35 ± 4.5%) (Fig. 4*D*).

ER–Mitochondria Coupling Is Affected Similarly by Other PS2 Mutants but Not by PS1 Mutants. Next, we wondered whether the effect on ER–mitochondria interactions is a specific property of PS2 over PS1. SH-SY5Y cells were transfected with the FAD-linked mutant PS1-A246E, and the effect on ER–mitochondria colocalization was investigated, as described in Fig. 3. Overexpression of PS1-A246E did not significantly increase the area of ER–mitochondria colocalization (+5.2 ± 7.2%, compared with control (mean ± SEM, $n = 28$) (Fig. S3 *A* and *B*). Consistently, down-regulation of endogenous PS1 by specific siRNA did not significantly modify ER–mitochondria tethering (+5.4 ± 6%; mean ± SEM; $n = 23$) Fig. S3 *D* and *E*). This latter observation further confirms that the results obtained with specific-PS2 siRNA were not caused by off-target effects.

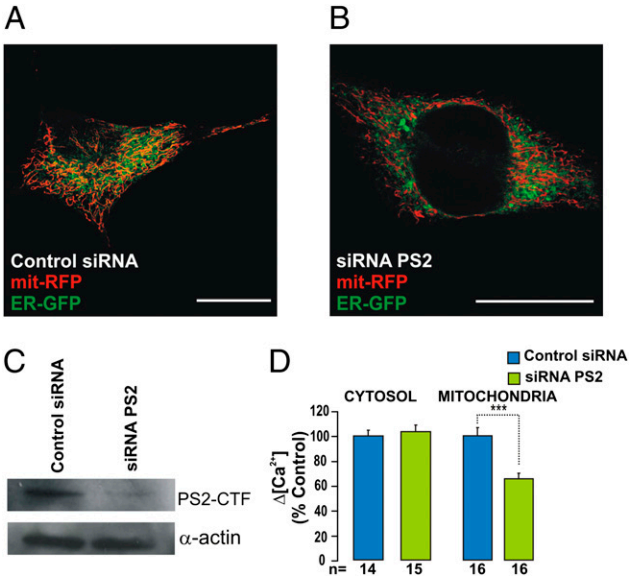

Fig. 4. Effect of endogenous PS2 on ER–mitochondria coupling. SH-SY5Y cells coexpressing mit-RFP and ER-GFP (or cyt/mit-Aeq) and treated with PS2-specific or control siRNA (20 nM) were analyzed by confocal microscopy (*A* and *B*) (Scale bar: 10 μm) to visualize the ER–mitochondria network, as described in Fig. 3 or by Western blotting (*C*) to check the expression level of PS2 (the PS2 C-terminal fragment, PS2-CTF, is shown). (*D*) The same cells were used to estimate the $[Ca^{2+}]_c$ and $[Ca^{2+}]_m$ responses (with aequorins) upon endogenous PS2 down-regulation with the protocol described in Fig. 1. Bars represent mean $[Ca^{2+}]_c$ (*Left*) and $[Ca^{2+}]_m$ (*Right*) peaks (mean ± SEM; ***$P < 0.001$; unpaired Student's *t* test; *n* = number of independent experiments).

In contrast, other PS2 mutants—i.e., the FAD-linked mutant PS2-N141I and the loss-of-function for γ-secretase activity mutant PS2-D366A, which also is devoid of endoproteolytic activity but is able to reduce $[Ca^{2+}]_{ER}$ (6)—strongly enhanced the extent of the ER–mitochondria interactions (increase of colocalization area: +33 ± 6.5%, $n = 21$, for PS2-N141I and +51 ± 6.8%, $n = 23$, for PS2-D366A; mean ± SEM; $P < 0.001$) (Fig. S4 *A–C*).

Finally, the effects on the $[Ca^{2+}]_c$ and $[Ca^{2+}]_m$ responses of these various mutants were investigated by aequorin measurements in SH-SY5Y cells. As previously reported for $[Ca^{2+}]_c$ and $[Ca^{2+}]_{ER}$ (6), both PS2-N141I and PS2-D366A mimicked the effect of PS2-T122R at the mitochondrial level (Fig. 1*C*). In particular, when predepleted cells were used as controls, a net, significant increase in mitochondrial Ca^{2+} uptake was observed (Fig. S4*G*). Down-regulation of endogenous PS1, although slightly increasing $[Ca^{2+}]_c$ rises, was without effect on $[Ca^{2+}]_m$ peaks (Fig. S3*F*, *Right*). Furthermore, treatment of controls with the γ-secretase inhibitors *N*-[*N*-(3,5-difluorophenacetyl)-L-alanyl]-*S*-phenylglycine *t*-butyl ester (DAPT) or L-685,458 (1 μM) was ineffective on both Ca^{2+} responses (Fig. S4*G*) and ER–mitochondria tethering (Fig. S4 *D–F*). In comparison with DMSO-treated cells (100 ± 5.1%; mean ± SEM; $n = 30$), the percentage changes of colocalization were −7 ± 6.9% and +14 ± 7.2% for DAPT ($n = 26$) and L-685,458 ($n = 24$), respectively, suggesting that the effect of PS2 on ER–mitochondria coupling is independent of its catalytic role within the γ-secretase complex. In sharp contrast, when the FAD-linked mutant PS1-A246E was overexpressed, neither cytosolic nor mitochondrial Ca^{2+} responses were changed (Fig. 1*C* and Fig. S3*F*, *Left*).

To test the possibility that the effect on ER–mitochondria tethering was caused by a reduced $[Ca^{2+}]_{ER}$, control cells incubated in a low-Ca^{2+} medium (50 μM) for 24 h were analyzed for their Ca^{2+} response, by aequorin, and for their ER–mitochondria interactions. With this treatment, cells showed a 30% reduction in $[Ca^{2+}]_c$ peak (71 ± 8.6%; $P < 0.01$; $n = 5$) compared with controls, a value similar to that obtained in the experiments of Fig. 1. These Ca^{2+}-depleted cells did not show an increase in ER–mitochondria interactions but rather a small, not significant, decrease (−15 ± 6.4% $n = 20$).

The specific effect of PS2 mutants on the mitochondrial Ca^{2+} response was independent of cell type, because it was observed in both rat cortical neurons (Figs. 2*C* and 3 *F–H*) and HeLa cells (Fig. S4*H*).

Overexpression or down-regulation of many proteins is known to modify the interactions of ER with mitochondria, but in most cases this effect is secondary to a massive modification of mitochondrial morphology. However, De Brito and Scorrano (25) recently have demonstrated that mitofusin2 (Mfn2) is expressed on both the outer mitochondrial membrane (OMM) and the ER, whereby it undergoes homotypic interactions and plays a direct role in mitochondria–ER tethering (25). We investigated the level of Mfn2 in controls and cells overexpressing either PS2 (WT or mutants) or PS1-A246E or with down-regulation of endogenous presenilins. Neither PS1 nor PS2 overexpression significantly modified Mfn2 protein level (Fig. S5*A*), whereas down-regulation of either endogenous PS1 or PS2 had a negative effect that was more pronounced for PS2 knockdown (Fig. S5*B*).

PS2-T122R Favors the Generation of Ca^{2+} Hot Spots on the OMM. The simplest explanation for the increased efficiency of mitochondrial Ca^{2+} uptake in cells expressing PS2 is that the augmented interactions between the two organelles influence the amplitude or the area of the Ca^{2+} hot spots generated close to mitochondria in response to ER Ca^{2+} mobilization (26). We recently demonstrated that N33D1cpv, a GFP-based probe on OMM, can monitor such hot spots quantitatively (22). SH-SY5Y cells

coexpressing N33D1cpv and PS2 (WT or T122R) or cotransfected with the void vector were challenged with a mixture of IP_3-generating agonists in a Ca^{2+}-free, EGTA-containing medium. Confirming the results of Fig. 2, we found that, of the 91 cells from seven independent experiments, the maximum mean peak ($\Delta R/R_0$), measured by the N33D1cpv probe was reached only by control cells. Furthermore, 23% of controls but 31% of the cells expressing WT PS2 and 60% of the cells expressing PS2-T122R showed a mean peak below 50% of the maximum value.

Fig. 5*A* shows that, in controls (blue diamonds), when the percentage of hot pixels was plotted as a function of the mean response of the cell, there was a positive correlation between the two parameters; i.e., a marginal number of hot pixels was found in cells with a mean peak increase 80% below the peak increase in the most-responding cells. This percentage increased as the average $\Delta R/R_0$ rose, as indicated by the correlation fit (dotted blue line). Compared with controls, a larger number of hot pixels was found in cells overexpressing PS2 (WT and T122R; yellow squares and red triangles, respectively); in addition, in cells overexpressing PS2 (especially PS2-T122R), such hot pixels were evident even in cells with a mean response well below 80% of the maximum average $\Delta R/R_0$ increase. As shown in the bar diagram of Fig. 5*B*, when the percentage of hot pixels was normalized to the mean response of each single cell, an increase in this parameter was found both for cells expressing PS2 WT and for cells expressing PS2-T122R (10.4 ± 4, $n = 20$; 23 ± 10.7, $n = 18$; and 33.6 ± 12.6, $n = 15$; $P < 0.05$, for controls, cells expressing PS2 WT, and cells expressing PS2–T122R, respectively). However, probably because of the large scattering of these data, the difference from controls was statistically significant only for PS2-T122R. Fig. 5*C* shows a 3D image of the distribution of hot pixels obtained in typical PS2-T122R cells (*Right*) and control cells (*Left*) with comparable average responses ($\Delta R/R_0 = 0.3$).

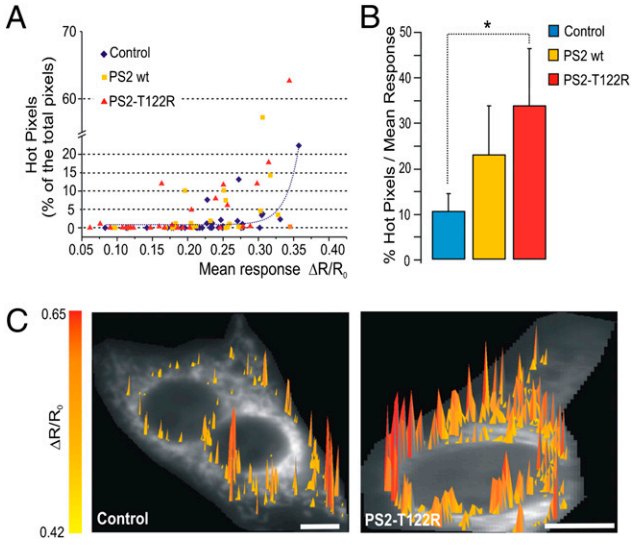

Fig. 5. Effect of PS2 overexpression on the generation of Ca^{2+} hot spots on the OMM. Cells are coexpressing N33D1cpv and: PS2 WT (yellow squares), PS2-T122R (red triangles), or void vector (controls; blue diamonds). Other conditions are as in Fig. 2. Hot pixels were evaluated as described in ref. 25 with some modifications (*SI Methods*). (*A*) Correlation between the percentage of hot pixels and the average ($\Delta R/R_0$) cell response. The correlation fit for control cells is shown (dotted blue line). (*B*) Bar diagram showing the percentage of hot pixels normalized to the mean response of each cell; only cells with hot pixels >0.1% were included (*SI Methods*). *$P < 0.05$; unpaired Student's *t* test. (*C*) 3D representation of the distribution of hot pixels in two cells with comparable average response ($\Delta R/R_0 = 0.3$): control cells (*Left*) and cells overexpressing PS2-T122R (*Right*). (Scale bar: 5 μm.)

Hot pixels of higher amplitude were clearly more abundant in the cells expressing mutant PS2.

Discussion

Presenilins are multifunctional proteins involved in different cellular functions, from the control of Notch signaling to the production of Aβ (27). Mutations in presenilins are responsible for most cases of early-onset FAD, although the pathogenic mechanism remains largely unknown. Much interest has been generated by the finding that presenilins can modulate different components of the Ca^{2+} signaling machinery, but contradictory results on this issue have been published by various groups (4).

Here we investigated the effects of transient expression or down-regulation of presenilins on ER–mitochondria interactions. The rationale for using transiently transfected cells, rather than cell clones or cells from transgenic animals, is twofold: Differences among clones may depend on intrinsic cell variability, and results in cells from transgenic animals may reflect adaptation phenomena and not the causal role of the protein of interest. We are aware of the limitations of experiments carried out in acutely transfected cells, and experiments in cells and tissues from transgenic mice expressing a FAD-linked PS2 mutant confirm and extend the results presented here.

The results appear clear-cut: Overexpression or down-regulation of WT or mutant PS1 has marginal effects on either the structural association or the efficacy of Ca^{2+} transfer between the ER and mitochondria. In contrast, modification in the level of PS2 potently modulates both processes. In particular, PS2 overexpression results in an increased tethering of the two organelles, whereas the opposite effect occurs upon PS2 down-regulation. As predicted, increases in PS2 level augment the efficacy of Ca^{2+} transfer from the ER to the mitochondria. Again, down-regulation of endogenous PS2 has the opposite effect.

Overexpression of PS2 WT has a smaller effect than overexpression of FAD-linked PS2 mutants on the association between the organelles (and therefore in favoring Ca^{2+} transfer). However, the role of endogenous PS2 is highlighted more easily upon down-regulation of the protein, using specific siRNA, that results in a very substantial reduction of both tethering and mitochondrial Ca^{2+} uptake. The effects of PS2 on ER–mitochondria interaction are observed not only in cell lines but also in primary cultures of rat cortical neurons.

For the hot spots generated at the OMM, we decided to use a more stringent criterion than applied previously (*SI Methods*), and, although the scattering of data is quite large, we observed an increased number of cells overexpressing PS2 (T122R in particular) presenting a large percentage of hot pixels, despite modest average $\Delta R/R_0$ rises.

The question then arises as to the mechanism by which PS2 modifies the interaction between the two organelles. We can conclude that the modulation of the ER–mitochondria interaction (*i*) does not require the enzymatic activity of PS2, (*ii*) does not require the presenilin endoproteolytic cut [because the equally effective PS2-D366A mutant also is devoid of this activity (28)], (*iii*) is not caused by ER Ca^{2+} overload or depletion, (*iv*) does not result from an increase of the intrinsic Ca^{2+} uptake capacity of mitochondria, and (*v*) does not correlate with modifications of Mfn2 levels.

The observation that the effects of PS2 overexpression (in WT or FAD-linked mutants) on SERCA, $[Ca^{2+}]_{ER}$ (6), and the mitochondria–ER connection are mimicked by a mutant devoid of catalytic activity suggests that all these effects depend on the level of full-length (FL) PS2. A similar conclusion was reached by Tu et al. (7). However, it should be mentioned that if FL PS2 WT formed Ca^{2+} leak channels, as suggested previously (7), the leak rate should be increased dramatically in cells overexpressing the protein, but the ER Ca^{2+} leak rate measured directly is increased only slightly (+15%) (6). Conversely, this latter finding is

more compatible with the model of an exaggerated Ca^{2+} release caused by PS2 modulation of the IP_3R opening probability (11, 12).

PS2 and PS1 are highly homologous, and their roles in cell functions often are considered to be largely overlapping. The present results, on the contrary, confirm and extend previous observations that, as far as Ca^{2+} handling is concerned, PS1 and PS2 have both similar and different roles. For example, both PS1 and PS2 overexpression in WT and FAD-linked mutants decrease $[Ca^{2+}]_{ER}$ (6) and increase Ca^{2+} leak across the ER (although to different extents), but only PS2 strongly inhibits SERCA activity (4, 6) and increases ER–mitochondria tethering. Of interest, along these lines, Behbahani et al. (29) showed that mitochondrial functions are reduced significantly in cells from PS2 (but not PS1) knockout animals. This energetic deficit could depend on the reduction of ER–mitochondria Ca^{2+} transfer, as elegantly demonstrated recently by Cárdenas et al. (30).

Although the present results provide information about the physiological role of PS2 in cellular Ca^{2+} homeostasis, the extrapolation of these data to the pathogenesis of FAD appears premature. However, alterations in the distance or number of contacts between ER and mitochondria may have profound impact on energetic metabolism (23, 31) as well as on the cellular response to Ca^{2+}-mediated cell-death stimuli (32). As far as FAD is concerned, a favored interaction between the two organelles may result in a chronic, toxic, mitochondrial Ca^{2+} overload that could contribute to neuronal metabolic dysfunction and ultimately cell death, thus being involved directly in the pathogenesis of the disease. Alternatively, an increase in ER–mitochondria tethering may mitigate the energetic defect linked to partial ER Ca^{2+} depletion caused by PS2 mutants, thus contributing to the milder phenotype of FAD cases linked to PS2 mutations.

Methods

Additional details are given in *SI Methods*.

Cell Culture and Transfection. SH-SY5Y and HeLa cells were grown and transfected as described (6). For RNAi experiments, the growth medium was replaced 1 h before transfection with antibiotic-free medium. siRNAs (mouse PS2, target sequence: GAUAUACUCAUCUGCCAUG; mouse PS1, target sequence: GGGAAGUAUUUAAGACCUA; siGENOME RISC-Free Control siRNA) (Dharmacon Research) were added to the transfection mixes to a final concentration of 20 nM.

Primary cultures of cortical neurons from postnatal day 0–1 Sprague–Dawley rats (Charles River Laboratories) were prepared, maintained, and transfected as described (20).

Aequorin Ca^{2+} Measurements. Aequorin measurements were carried out as described (6) and are summarized in *SI Methods*. To deplete the ER Ca^{2+} content partially, cells were preincubated for fixed time intervals (5–60 min) in Ca^{2+}-free, EGTA-containing medium (600 μM) at 4 °C or in Ca^{2+} medium at 37 °C with the cell-permeable Ca^{2+} chelator EGTA acetoxymethyl ester (EGTA-AM) (10 μM). Varying the EGTA-AM incubation time resulted in a more reproducible decrease in Ca^{2+} peaks than achieved by changing the EGTA-AM concentration at a fixed loading time.

Fluorescence Ca^{2+} Imaging. SH-SY5Y cells and neurons expressing H2BD1cpv and 4mtD1cpv were analyzed as previously described (22) and as summarized in *SI Methods*.

Materials. CPA, histamine, ATP, BK, ionomycin, and digitonin were purchased from Sigma-Aldrich. All other materials were analytical or highest available grade. EGTA-AM was from Invitrogen.

Statistical Analysis. All data are representative of at least five different experiments. Data were analyzed using Origin 7.5 SR5 (OriginLab Corporation) and ImageJ (National Institutes of Health,). Averages are expressed as mean ± SEM.

ACKNOWLEDGMENTS. We thank P. Capitanio and R. Filadi for performing some of the experiments, R. Tsien for the cDNA coding for D1cpv, and P. Magalhães for useful suggestions. This work was supported by the Fondo per gli Investimenti della Ricerca di Base (FIRB) Grant RBIN042Z2Y (to P.P.), by grants from the Italian Ministry of University and Research (to C.F., P.P., and T.P.), and by grants from the Veneto Region, the Italian Institute of Technology, the Strategic Projects of the University of Padua, and the Fondazione Cassa di Risparmio di Padova e Rovigo (CARIPARO) Foundation (to T.P.). M.J.K. is the recipient of a Ph.D. fellowship from the CARIPARO Foundation.

1. Goedert M, Spillantini MG (2006) A century of Alzheimer's disease. *Science* 314: 777–781.
2. Bojarski L, Herms J, Kuznicki J (2008) Calcium dysregulation in Alzheimer's disease. *Neurochem Int* 52:621–633.
3. Mattson MP (2010) ER calcium and Alzheimer's disease: In a state of flux. *Sci Signal* 3: pe10.
4. Zampese E, Brunello L, Fasolato C, Pizzo P (2009) Ca^{2+} dysregulation mediated by presenilins in familial Alzheimer's disease: Causing or modulating factor? *Curr Trends Neurol* 3:1–14.
5. Green KN, et al. (2008) SERCA pump activity is physiologically regulated by presenilin and regulates amyloid beta production. *J Cell Biol* 181:1107–1116.
6. Brunello L, et al. (2009) Presenilin-2 dampens intracellular Ca^{2+} stores by increasing Ca^{2+} leakage and reducing Ca^{2+} uptake. *J Cell Mol Med* 13(9B):3358–3369.
7. Tu H, et al. (2006) Presenilins form ER Ca^{2+} leak channels, a function disrupted by familial Alzheimer's disease-linked mutations. *Cell* 126:981–993.
8. Nelson O, et al. (2007) Familial Alzheimer disease-linked mutations specifically disrupt Ca^{2+} leak function of presenilin 1. *J Clin Invest* 117:1230–1239.
9. LaFerla FM (2002) Calcium dyshomeostasis and intracellular signalling in Alzheimer's disease. *Nat Rev Neurosci* 3:862–872.
10. Thinakaran G, Sisodia SS (2006) Presenilins and Alzheimer disease: The calcium conspiracy. *Nat Neurosci* 9:1354–1355.
11. Cheung KH, et al. (2008) Mechanism of Ca^{2+} disruption in Alzheimer's disease by presenilin regulation of $InsP_3$ receptor channel gating. *Neuron* 58:871–883.
12. Cheung KH, et al. (2010) Gain-of-function enhancement of IP3 receptor modal gating by familial Alzheimer's disease-linked presenilin mutants in human cells and mouse neurons. *Sci Signal* 3:ra22.
13. Green KN, LaFerla FM (2008) Linking calcium to Abeta and Alzheimer's disease. *Neuron* 59:190–194.
14. Area-Gomez E, et al. (2009) Presenilins are enriched in endoplasmic reticulum membranes associated with mitochondria. *Am J Pathol* 175:1810–1816.
15. Hayashi T, Rizzuto R, Hajnoczky G, Su TP (2009) MAM: More than just a housekeeper. *Trends Cell Biol* 19:81–88.
16. Celsi F, et al. (2009) Mitochondria, calcium and cell death: A deadly triad in neurodegeneration. *Biochim Biophys Acta* 1787:335–344.
17. Su B, et al. (2010) Abnormal mitochondrial dynamics and neurodegenerative diseases. *Biochim Biophys Acta* 1802:135–142.
18. Swerdlow RH, Burns JM, Khan SM (2010) The Alzheimer's disease mitochondrial cascade hypothesis. *J Alzheimers Dis* 20(Suppl 2):S265–S279.
19. Santos RX, et al. (2010) Alzheimer's disease: Diverse aspects of mitochondrial malfunctioning. *Int J Clin Exp Pathol* 3:570–581.
20. Zatti G, et al. (2006) Presenilin mutations linked to familial Alzheimer's disease reduce endoplasmic reticulum and Golgi apparatus calcium levels. *Cell Calcium* 39:539–550.
21. Pinton P, Leo S, Wieckowski MR, Di Benedetto G, Rizzuto R (2004) Long-term modulation of mitochondrial Ca^{2+} signals by protein kinase C isozymes. *J Cell Biol* 165: 223–232.
22. Giacomello M, et al. (2010) Ca^{2+} hot spots on the mitochondrial surface are generated by Ca^{2+} mobilization from stores, but not by activation of store-operated Ca^{2+} channels. *Mol Cell* 38:280–290.
23. Rizzuto R, Pozzan T (2006) Microdomains of intracellular Ca^{2+}: Molecular determinants and functional consequences. *Physiol Rev* 86:369–408.
24. Manders EMM, Verbeek FJ, Aten JA (1993) Measurement of co-localization of object in dual-colour confocal images. *J Microsc* 169:375–382.
25. de Brito OM, Scorrano L (2008) Mitofusin 2 tethers endoplasmic reticulum to mitochondria. *Nature* 456:605–610.
26. Rizzuto R, et al. (1998) Close contacts with the endoplasmic reticulum as determinants of mitochondrial Ca^{2+} responses. *Science* 280:1763–1766.
27. Wakabayashi T, De Strooper B (2008) Presenilins: Members of the gamma-secretase quartets, but part-time soloists too. *Physiology (Bethesda)* 23:194–204.
28. Walker ES, Martinez M, Brunkan AL, Goate A (2005) Presenilin 2 familial Alzheimer's disease mutations result in partial loss of function and dramatic changes in Abeta 42/40 ratios. *J Neurochem* 92:294–301.
29. Behbahani H, et al. (2006) Differential role of Presenilin-1 and -2 on mitochondrial membrane potential and oxygen consumption in mouse embryonic fibroblasts. *J Neurosci Res* 84:891–902.
30. Cárdenas C, et al. (2010) Essential regulation of cell bioenergetics by constitutive InsP3 receptor Ca2+ transfer to mitochondria. *Cell* 142:270–283.
31. Hajnóczky G, Robb-Gaspers LD, Seitz MB, Thomas AP (1995) Decoding of cytosolic calcium oscillations in the mitochondria. *Cell* 82:415–424.
32. Scorrano L, et al. (2003) BAX and BAK regulation of endoplasmic reticulum Ca^{2+}: A control point for apoptosis. *Science* 300:135–139.